Microparticle characterization using digital holography

Emmanouil Darakis [a,b], Taslima Khanam [a], Arvind Rajendran [a,*], Vinay Kariwala [a], Thomas J. Naughton [b,c], Anand K. Asundi [d]

[a] Nanyang Technological University, School of Chemical and Biomedical Engineering, Singapore 637459, Singapore
[b] National University of Ireland Maynooth, Department of Computer Science, Maynooth, County Kildare, Ireland
[c] University of Oulu, RFMedia Laboratory, Oulu Southern Institute, Vierimaantie 5, 84100 Ylivieska, Finland
[d] Nanyang Technological University, School of Mechanical and Aerospace Engineering, Singapore 639798, Singapore

ARTICLE INFO

ABSTRACT

Digital holography is an effective 3D imaging technique, with the potential to be used for particle size measurements. A digital hologram can provide reconstructions of volume samples focused at different depths, overcoming the focusing problems encountered by other imaging based techniques. Several particle analysis methods discussed in the literature consider spherical particles only. With the object sphericity assumption in place, analysis of the holographic data can be significantly simplified. However, there are applications, such as particle analysis and crystallization monitoring, where non-spherical particles are often encountered. This paper discusses the processing of digital holograms for particle size and shape measurement for both spherical and arbitrarily shaped particles. An automated algorithm for identification of particles from recorded hologram and subsequent size and shape measurement is described. Experimental results using holograms of spherical and non-spherical particles demonstrate the performance of the proposed measuring algorithm.

© 2009 Elsevier Ltd. All rights reserved.

1. Introduction

The size and shape in many cases, govern the properties of particulate matter (Winn and Doherty, 2000). Characterizing these properties accurately is an important step towards tailoring them to suit process and product requirements. Although the measurement of particle size is a mature technique, shape measurement is rather new. Advancements in imaging based techniques (for example, particle vision measurement) has made it possible to obtain both size and shape of particles through 2D imaging tools followed by the use of an image processing algorithm. Online measurement techniques are also being continuously investigated (Ruf et al., 2000; Abbas et al., 2002; Patience and Rawlings, 2001; Larsen et al., 2007; Wang et al., 2008). The techniques based on 2D imaging systems suffer from limited depth of focus imposed by the required magnification. As a consequence, captured images contain blurred and out-of-focus objects limiting the successful application of image analysis (Larsen et al., 2007; Wang et al., 2008). Hence there is a strong need to develop online sensors and imaging tools capable of providing accurate size and shape information of a population of particles.

Holographic particle analysis has been reported as an effective technique for measurement of the position, size distribution, and speed of particles or other micro-objects suspended in fluids (Vikram, 1992). It provides 3D volume information from a single hologram acquisition. The actual location of the particle can be determined subsequently by reconstructing the recorded hologram at different depths. Thus holography does not encounter the problem of out-of-focus particles as classical imaging tools. In comparison with classical film based holography, the use of digital holography is more attractive due to the ease of set-up and recording process using a digital camera (Schnars and Juptner, 2005; Frauel et al., 2006; Asundi and Singh, 2006). The application of digital holography for particle analysis has been discussed in literature (Xu et al., 2002; Schnars and Juptner, 2005; Asundi and Singh, 2006). Similar techniques have been used for several applications including the study of plankton in sea water (Sun et al., 2007) and holographic particle image velocimetry (Hinsch, 2002).

In this work, we benchmark digital holographic microscopy for measurement of particle size distribution of a population of microparticles. For this purpose, we use non-crystalline opaque microparticles, which are representative of particles encountered in real particle characterization situations. In particular, we investigate two classes of particles, namely spheres and fibers which represent the extremes of particle shapes encountered in real world situations, i.e. spheres and needles and are hence ideal for benchmarking.

* Corresponding author. Tel.: +65 63168813; fax: +65 67947553.
  E-mail address: arvind@ntu.edu.sg (A. Rajendran).

An algorithm is required for processing digital holograms to extract size and shape information. Although fringe analysis based methods are available for estimating the size or the focusing point of particles recorded in digital holograms without reconstruction (Onural and Ozgen, 1992; Buraga-Lefebvre et al., 2000; Denis et al., 2006; Soontaranon et al., 2008), these methods assume spherical shape of particles and hence are not applicable for the measurement of other shapes.

In this paper, we propose an algorithm that uses hologram reconstructions at several depths to extract size and shape information. In this algorithm, particles are segmented from the background using Canny edge detection (Canny 1986) and best focusing depth for each particle is identified based on a focusing metric. The size and shape information are extracted using the reconstructed image at the best focusing depth. The proposed algorithm is automated, but has a few tuning parameters. The performance of the algorithm, however, is not very sensitive to the choice of tuning parameters. This is verified by applying the proposed algorithm to experimentally recorded holograms of particles with different shapes (spherical and needle shaped), size ranges (10 μm − few hundred μm) and experimental conditions (static, suspension, and flow-through). In every case, the particle size distributions (PSD) measured by the algorithm closely matches with the expected PSD. In summary, this paper successfully establishes digital holography as a technique for accurate measurement of PSD and opens up avenues for potential applications to particle characterization and analysis.

The rest of the paper is organized as follows: In Section 2, the principles of holography, recording setup and fundamentals of digital holography are discussed. In Section 3, the algorithm used for the processing of the recorded digital holograms is described. In Section 4, the experiments used to verify the accuracy and the effectiveness of the algorithm are presented and Section 5 concludes the paper.

2. Holography and holograms

2.1. Principle

Holography is an optical phenomenon based on the fundamental theory of diffraction and interference. To explain this phenomenon, a typical optical set-up for traditional free-space in-line digital holographic microscopy, shown in Fig. 1(a), is used. In this configuration, a strongly coherent light source (laser) illuminates an object. A part of the light is diffracted by the

object creating the "object beam", while another part, called "reference beam" remains undiffracted. The object and reference beams interfere with one another and form an interference pattern which is recorded by a light sensitive medium, e.g. photographic film (Schnars and Juptner, 2005). The recorded interference pattern is called a hologram. When the hologram recorded by the photographic film (after subsequent chemical film development) is illuminated by the original reference wave in the absence of the object, it enables the reconstruction of the original object beam at the previous object position as shown in Fig. 1(b). The reconstruction results in a virtual image of the original object which exhibits the effects of perspective and depth of focus. Hence, in comparison with other 2D imaging techniques, holography offers a unique characteristic of restoring 3D volume information from a single hologram acquisition (Schnars and Juptner, 2005).

Classical film based holography provides high resolution hologram recording, but suffers from an increased processing time required for the cumbersome recording and subsequent chemical film development for reconstruction process. The use of charged couple device (CCD) as the holographic recording medium makes the technique more attractive by eliminating the aforesaid complications associated with classical film based holography. This technique, termed digital holography, provides the possibility to perform reconstructions numerically, which has several advantages, as illustrated in the next section.

2.2. Digital in-line holographic microscopy

Fig. 2 shows the schematic of the digital in-line holography setup used to record the holograms. The setup consists of a laser source and a microscope objective lens that focuses the laser beam on a pinhole located at a distance D from the recording camera. The sample which is located at a distance d from the recording camera is illuminated by the resulting spherical diverging beam. One part of the illuminating beam passes through the sample undiffracted and acts as the reference beam. The other part of the illuminating beam is diffracted by the particles within the sample generating the object beam. The interference pattern created by the object and the reference beam, called as the hologram, is recorded by the recording camera. Fig. 3(a) shows an example of a digital hologram of a population of polymer spheres suspended in water.

The reconstruction of the scene at a desired distance can be obtained by multiplying the recorded interference pattern with the reference wave and propagating it through a Fresnel–Kirchhoff integral that can be evaluated numerically using the convolution method (Schnars and Juptner, 2005). Figs. 3(b) and (c) show sample reconstructions, at two different depths, obtained from the hologram shown in Fig. 3(a). As can be seen, objects at different positions along the z axis (optical axis) come into focus as d changes. It is worth emphasizing that the two reconstructions
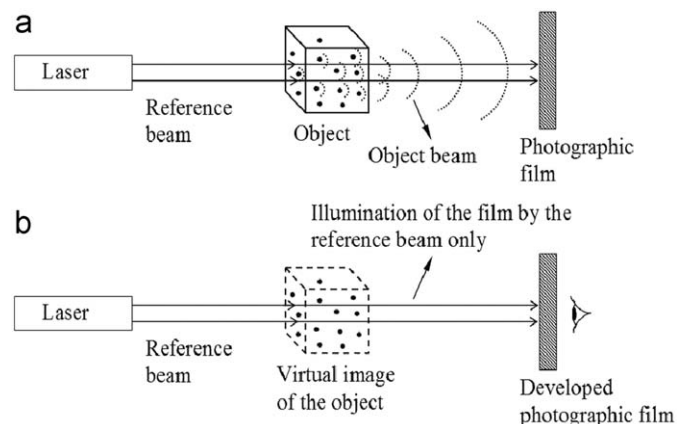

Fig. 1. Principle of holography: (a) a typical set-up for recording of a hologram; solid lines correspond to reference beam and dotted curves correspond to object beam. (b) Reconstruction of the hologram.
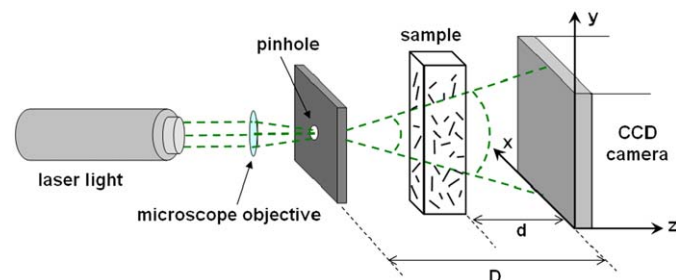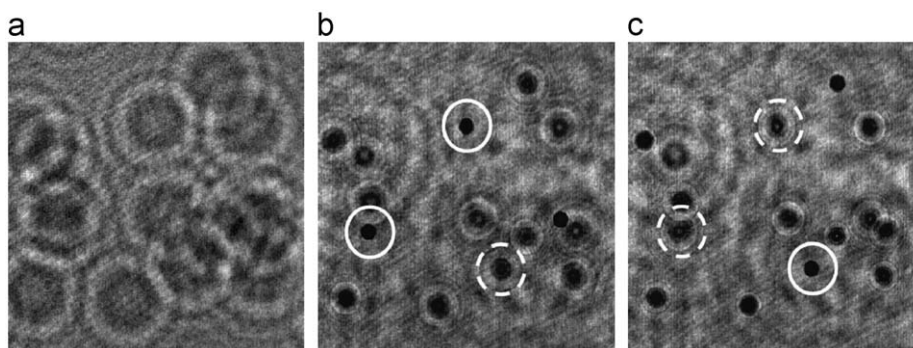

Fig. 2. Schematic of an in-line digital holographic recording setup.

Fig. 3. Digital holographic microscopy of polymer spheres suspended in water (a) hologram; (b) a sample reconstruction at distance d_1; (c) reconstruction at a different distance d_2. Solid circles indicate particles focused at the chosen reconstruction depth.

are obtained from the same hologram and hence it is possible to overcome the focusing issue that is encountered in classical imaging techniques. This is an unique advantage of holography. It is worth noting that the diverging beam used in the current set-up introduces a magnification. This magnification, which is a function of the reconstruction distance, has to be properly accounted for in order to perform quantitative measurements from the reconstructed images (Schnars and Juptner, 2005; Vikram, 1992).

## 3. Digital hologram processing for particle measurements

There are several algorithms available for extraction of particle properties, such as size and location, from the hologram without reconstruction (Buraga-Lefebvre et al., 2000; Denis et al., 2006; Soontaranon et al., 2008). These algorithms, however, assume that the particles are spherical and hence cannot be used for accurate size and shape measurement of non-spherical particles. In this section, we propose a method for obtaining the particle information from reconstructions of recorded hologram at several depths. For easier illustration, the overall algorithm is pictorially represented in Fig. 4. Details of the proposed algorithm for processing the hologram and subsequent image analysis for particle characterization are discussed in the following sections.

3.1. Numerical reconstruction

Naturally, the first step after hologram acquisition, is reconstruction of the hologram at several depths. The distance between successive reconstructions depends on the minimum size of the particles to be studied and the depth resolution of the system. In general, this distance should be similar to the minimum particle size that needs to be identified, if not smaller.

3.2. Image segmentation

A possible approach for image segmentation involves thresholding the intensity of the reconstruction (Malkiel et al., 2004). In threshold based segmentation, pixels with intensity value lower than the threshold are considered to belong to a particle, while pixels with intensity values higher than the threshold are considered to be background (Calderon De Anda et al., 2005; Sarkar et al., 2009). In general, the selection of an appropriate threshold value can be difficult. An inappropriate choice for threshold value results in identification of noise, e.g. impurities in the sample solution, speckle noise from the laser, diffraction effects from multiple objects, etc., present in reconstructed
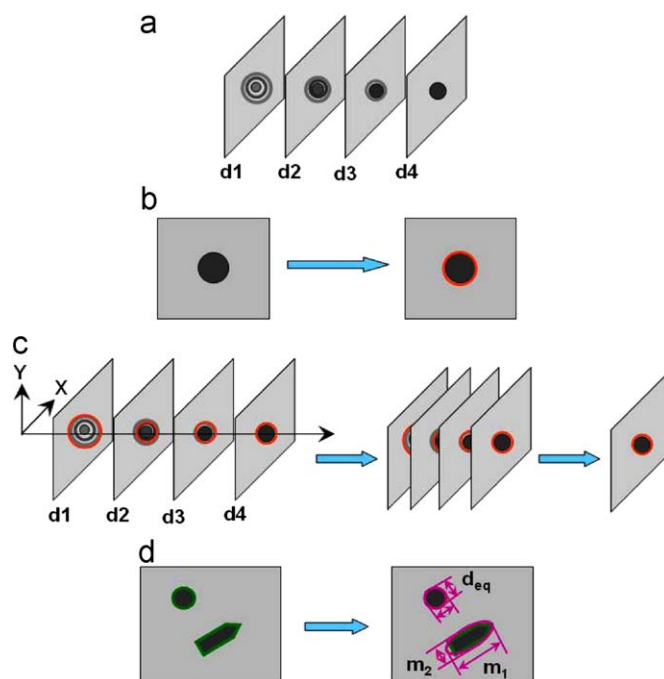
Fig. 4. Steps of hologram processing algorithm. (a) Numerical reconstruction at several depths; (b) image segmentation using Canny edge detection; (c) localization of a particle; and (d) particle size and shape measurement, d_{eq} denotes the equivalent diameter for spherical objects, while m_1 and m_2 represent the major and minor axes for non-spherical objects.

holograms as particles or unidentified particles. Furthermore, imperfections such as non-uniform illumination of the hologram lowers the performance of threshold based segmentation. Some additional details regarding the drawbacks of threshold based segmentation are given elsewhere (Darakis et al., 2008; Khanam et al., 2008).

In this paper, we use the Canny edge detection (Canny 1986) technique for particle segmentation. In this technique, a Gaussian filter with standard deviation, σ, is first applied to the reconstruction to reduce the effect of noise. Subsequently, the edges are detected by examining the gradients of intensity for local maxima. Here, thresholding with hysteresis is used to classify the identified maxima using two threshold values, t_L and t_H ($t_H > t_L$). Maxima with a value lower than t_L are identified as not being edges. Similarly, maxima with a value higher than t_H are identified as edges. Maxima with value between t_L and t_H are identified as edges only if they are connected to identified edges (Sarkar et al.,

2009). Apart from good localization, the use of edge detection-based particle segmentation on digital holograms also has the advantage that highly unfocused particles are not detected, as particles are usually surrounded by strong edges only close to their best focusing point.

For every reconstruction, the edge detection algorithm results in a binary matrix with ones corresponding to pixels where edges are detected and zeros elsewhere. To identify particles from this matrix, dark areas completely enclosed by edges are filled to form blobs, which are considered as possible particles. Open ended lines are removed by erosion followed by dilation in order to eliminate noisy formations that frequently appear in the background. This, in principle, does not change the size of the identified blobs. To avoid identifying noise as particles, blobs with diameter less than a cut-off value are removed. Further, blobs touching the edges of the reconstruction window are also removed, as these particles are partially located outside the reconstruction. Finally, a set of blobs corresponding to particles detected in the reconstruction under consideration is obtained.

The edge detection algorithm requires the selection of three parameters: the standard deviation of the filter, σ, and the two thresholds, t_L and t_H. A large σ value results in a Gaussian filter with large width, which may affect the size of small particles causing erroneous size measurements. Thus, σ is selected such that the filtering operation does not alter the size of the particles under investigation. On the other hand, the thresholds t_L and t_H only affect the number of identified particles and not their sizes. High values lead to identification of fewer particles (particles with very sharp edges), while lower values lead to false positives (areas surrounded by sharp edges). The false positives correspond to fringes caused by the twin image or out of focus particles and are much brighter than focused particles. As a result, they can be easily identified and neglected based on their average intensity. The performance of the algorithm is not very sensitive to the selection of these parameters. In this paper, t_L and t_H are chosen as 0.3 and 0.6, respectively, and the same set of parameters has been used for the different experimental results presented in Section 4 and were found to give good results for holograms recorded under different conditions and containing particles of different size ranges.

3.3. Localization of a particle

As the particle segmentation step is applied to every reconstruction of the hologram, a single particle may be identified in several reconstructions. Further, the magnification depends on the reconstruction distance. Thus, the best focusing depth needs to be determined for accurate size and shape measurement, i.e. particle localization has to be performed.

To find the best focusing depth, blobs with overlapping spatial positions at different reconstruction depths are given identical labels. Subsequently, the mean intensity and the variance of each blob is calculated. The reconstruction depth at which these parameters show a minimum is taken as the best focused depth. Particles with minimum of the focusing metric occurring at the first or last examined depth, are likely to be located outside the examined depth range and hence are ignored to avoid erroneous measurements.

The determination of focusing metric has been independently verified (Darakis et al., 2008). In the verification experiments several ceramic beads (average diameter 80 μm) were positioned on a glass slide which was placed on a movable mount. The slide was then positioned at a known distance along the optical axis and the best focused depth was calculated according to the algorithm mentioned above. It was found that the maximum observed error between the measured and expected slide position was 120 μm over a scanned depth of 14 mm. This translates into a 0.35% error in the magnification, which is negligible.

3.4. Particle size and shape measurements

Particle segmentation and focusing provide the area occupied by each particle at its best focusing depth. In general, the particles are not spherical and thus the identified regions are not circular. As a result, it is not always easy to measure their sizes. Although several metrics are available for characterizing non-spherical particles, we limit ourselves to the following two as they represent quantities that are easy to measure and are capable of classifying particle shape:

(1) *Equivalent diameter*, corresponding to the diameter of a circle with the same area as the identified area. This parameter is used for the systems that are spherical, or close to spherical.
(2) *Major and minor axes length*, corresponding to axis lengths of an ellipse with the same normalized second central moment as the identified area. This metric is used for non-spherical particles that have one characteristic length sufficiently longer than the others (Kempkes et al., 2008).

Naturally, the distribution of equivalent diameter corresponds to the particle size distribution (PSD) of particles, if the particles are spherical.

As mentioned earlier, the system introduces magnification. Thus, the measured values (equivalent diameter and axes lengths) need to be converted to true values using the magnification factor M as

$$r = \frac{r_{pixels} \Delta x}{M(d_0)}, \tag{1}$$

where r_{pixels} is the measured size of the particle in pixels, Δx the size of a pixel on the CCD camera, and d_0 is the best focusing depth of each particle.

4. Experiments and results

In this section, several experiments are presented to verify the performance of algorithm described in Section 3. In these experiments, the recording setup shown in Fig. 2 was used. The setup uses a laser source with a wavelength $\lambda = 532$ nm. A $60\times$ microscope objective lens focuses the laser beam on a 1 μm pinhole located at a distance $D = 63.3$ mm from the recording camera (The Imaging Source DMK41BF02, Bremen, Germany), with $N_x \times N_y = 1280 \times 960$ monochrome pixels measuring 4.65×4.65 μm each. The threshold values and the standard deviation of the Gaussian filter were chosen as $t_L = 0.3$, $t_H = 0.6$, and $\sigma = 1.5$, respectively. These parameters were retained for all experimental systems listed in Table 1.

The experiments were designed to achieve two primary goals. Firstly, to demonstrate the applicability of digital holography for

Table 1
Characteristics of various particles used in the holography measurements.

Experimental system	Average size	Shape
Ceramic beads on glass slide	Diameter ≈ 80 μm	Spherical to elliptical
Polymer particles in flow-through system	Diameter 40 μm	Spherical
Carbon fibers	Diameter ≈ 8 μm, length $\approx 50-500$ μm	Needle
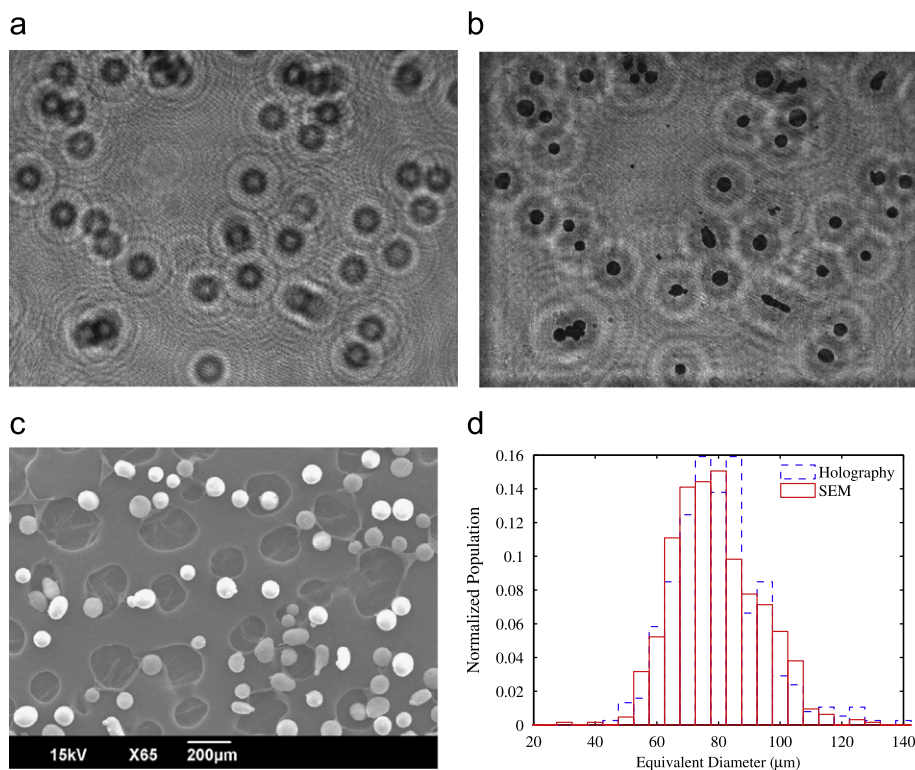
Fig. 5. Digital holographic microscopy data of ceramic beads on glass slide: (a) one of the recorded digital holograms, (b) example of a reconstructed image, (c) example of an SEM image of ceramic beads. Bright areas correspond to particles whereas dark circular areas on the background are irregularities of the sample holder. (d) Comparison of PSD obtained from digital holography and SEM.

size and shape measurement of populations of spherical and non-spherical particles. Secondly to demonstrate this under situations that are encountered in practice, namely dry and wet (particles suspended in solution) conditions and flowing suspensions. The results are presented in order of the complexity of the measurement scenario. Firstly, characterization under dry and wet condition of spherical particles are presented. Then the measurement of needle shaped particles on a glass slide and in suspension is presented.

4.1. Ceramic beads on glass slide

In order to verify the performance of the particle measurement algorithm, ceramic beads (Microbeads AG, Switzerland) placed on a glass slide were used. The slide was positioned normal to the optical axis and a hologram was recorded. This procedure was repeated several times to account for a population of particles. Fig. 5(a) shows one of the recorded holograms and Fig. 5(b) shows a sample reconstruction. A total of 31 holograms were processed using the procedure described in Section 3. Here, a depth of 3 mm with a step size of 50 μm was used for each hologram resulting in identification of 377 different particles.

In addition, scanning electron microscopy (SEM) was used to record several images of particles taken from the same population. One such image is shown in Fig. 5(c). To segment the SEM images and extract particles (bright areas), Canny edge detection was used with the same parameters as used for the segmentation of reconstructed holograms. The focusing was performed manually during the recording and the size of each particle was measured considering the magnification of the SEM. Overall, 615 different particles were measured from the SEM captured images.

Fig. 5(d) shows the resulting distributions of equivalent diameters of ceramic beads obtained from the holography and the SEM experiments. The mean particle size identified from

the holographic microscopy and the SEM are $80.24 \pm 14.46\,\mu m$ (mean $\pm$ standard deviation) and $79.23 \pm 13.79\,\mu m$, respectively, showing good agreement. Hence, this experiment verified the accuracy of the digital holography based measurement algorithm.
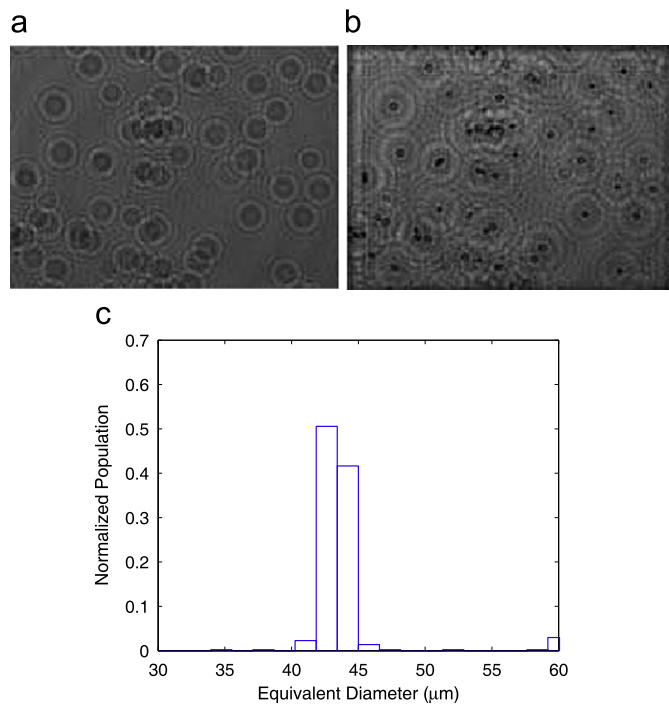
4.2. Polymer particles in flow-through system

For this experiment, the object used in the set-up consisted of a flow cell with flowing particle suspensions. National Institute of Standards and Technology (NIST) certified polymer microspheres manufactured by Duke Scientific Corporation, USA with diameter of $40.25 \pm 0.32\,\mu m$ were continuously pumped from a beaker through circulation loop using a peristaltic pump. The particles flowed through a quartz flow cell with dimensions 12.5 mm (L) × 12.5 mm (W) × 65 mm (H) and optical path length of 10 mm at a flow rate 5 mL/min. Holograms were captured at the rate of one hologram per second. Reconstructions were carried out with a distance of 50 μm between each other covering a volume with a depth of 8 mm.

Fig. 6(a) shows one of the recorded holograms for the polymer particles and a sample reconstruction is shown in Fig. 6(b). By analyzing nine holograms, the algorithm identified 437 different particles. The resulting distribution of equivalent diameter is shown in Fig. 6(c). The obtained mean particle size was $43.89 \pm 3.38\,\mu m$. There is an error of $\approx 4\,\mu m$ between the actual and measured particle size, which is below the resolution limit of the system ($\approx 7\,\mu m$). In Fig. 6(c), the presence of particles with diameter $\approx 60\,\mu m$ can also be noted. This indicates the presence of agglomerated particles.

4.3. Characterization of fibers

The measurement of fibers deserves special attention. Unlike the case of spheres, where each particle is best focused on a

Fig. 6. Size measurements for polymer particles in flow-through system: (a) hologram; (b) sample reconstruction; (c) distribution of equivalent diameter. Measured mean equivalent diameter is $43.89 \pm 3.38 \, \mu m$ where as expected mean diameter is $40.25 \pm 0.32 \, \mu m$.

particular plane, the case of fibers is not straightforward. Fibers that lie orthogonal to the optical axis, will be focused at a particular depth. However, for fibers that are not orthogonal to the optical axis, only a part of the fiber will be focused at particular depth. Under these situations, the algorithm would measure only the length of their projections on the reconstruction plane. In order to study this, the first set of experiments involved the measurement of a single fiber placed on a glass slide. In the second set of experiments, measurements of a population of fibers in a solution are reported. In these experiments, particles with needle shape were studied using carbon fibers (TOHO Tenax Type 383) suspended in water.

4.3.1. Single fiber on a glass slide

In the first set of experiments, a single fiber was placed on a glass slide connected to a rotatable mount that can be adjusted to obtain a desired out-of-plane tilt. Two fibers with lengths 150 and $1320 \, \mu m$, respectively, were allowed to rotate from $0°$ to $55°$ tilt at $5°$ interval with respect to the optical axis. The holograms were processed according to the algorithm discussed earlier. Since the fibers are clearly non-spherical, the major and minor axes obtained by fitting an ellipse were used to characterize the sizes. It is worth noting that while the fibers are rectangular, fitting an ellipse leads to an over prediction of the axis lengths. Hence, the measured lengths of the major and minor axes are multiplied by a factor of $\sqrt{3}/2$ to convert them to fiber length and diameter, respectively (Eggers et al., 2008).

Based on the length and the angle of tilt the expected projected length, as shown by the continuous lines in Figs. 7(a) and (b), can be calculated. The comparison between the measured and calculated projected lengths is shown in Fig. 7(a). As it can be seen the algorithm successfully estimated the projected length of the $150 \, \mu m$ long fiber within the expected accuracy even for large out-of-plane tilts. For the $1320 \, \mu m$ long fiber, the algorithm
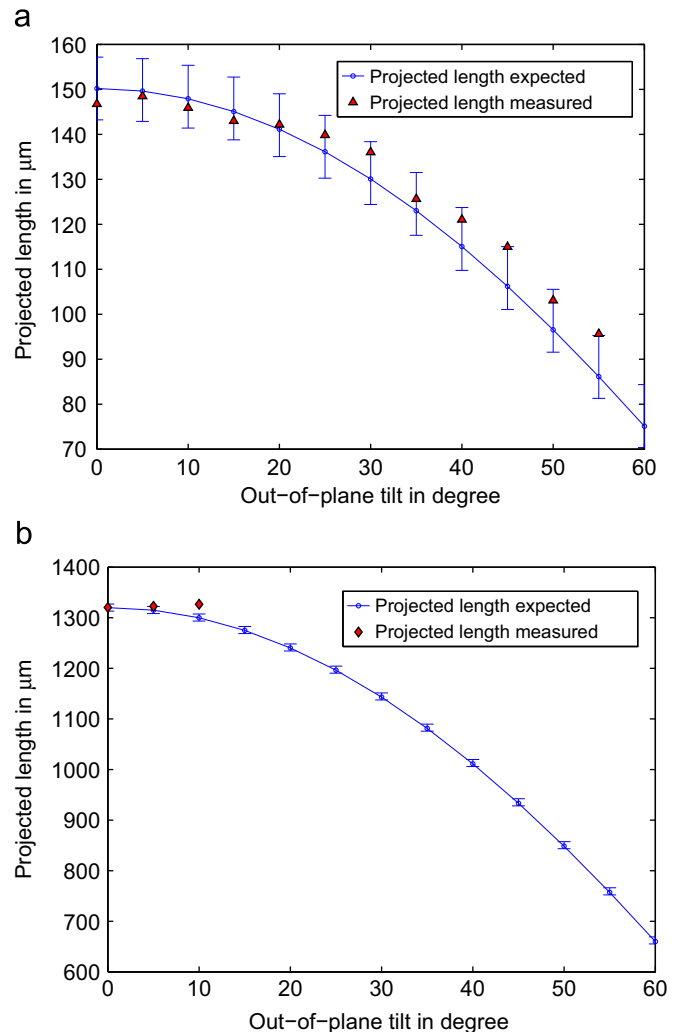
Fig. 7. Measurement accuracy of the algorithm for fibers for out-of-plane tilt: (a) $150 \, \mu m$ long fiber; (b) $1320 \, \mu m$ long fiber. The error bars take into account the system resolution and the uncertainty in the measurement of the tilt.

measured the fiber only for small tilts (cf. Fig. 7(b)). For higher tilts, long fibers are not entirely focused on a single reconstruction and hence the algorithm neglects such fibers, as they are not enclosed by strong edges. In this way, erroneous measurements are avoided but false negatives are introduced. It is worth pointing out that in the case of fibers the measured lengths that are eventually identified correspond not to the real lengths but only the projected lengths. In this case rigorous comparison with other measurements is difficult, unless complex inversion techniques to convert projected lengths to real lengths for a population of particles are considered (Eggers et al., 2008). To overcome the limitation associated with long tilted fibers as well as complex inversion techniques to convert projected lengths to real lengths, we recently developed a technique to measure the real lengths of fibers from hologram reconstructions directly without a priori knowledge of fiber tilt, position and length (Kempkes et al., 2009). However, it is computationally intensive and its applicability to fibers shorter than $\approx 200 \, \mu m$ needs to be improved. Hence, this technique is not applied in this work.

4.3.2. Carbon fibers suspended in water

Based on the understanding gained from the first set of experiments, measurements were performed with a population of
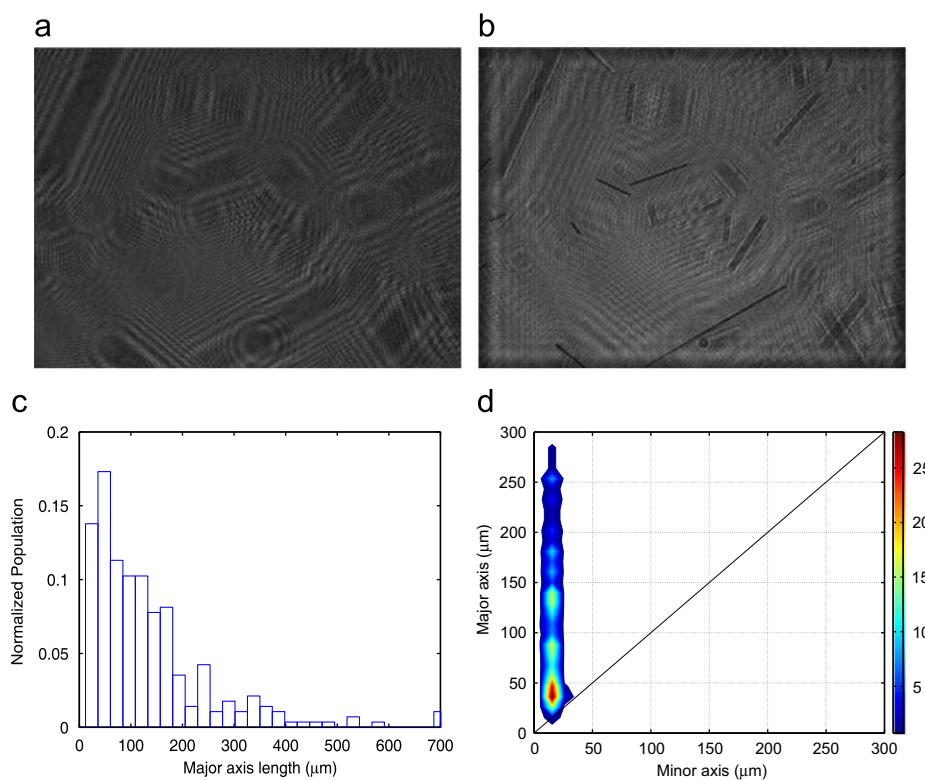
Fig. 8. Size measurements for carbon fibers suspended in water: (a) hologram; (b) sample reconstruction; (c) major axis length distribution; (d) axis length distribution.

carbon fibers contained in a quartz cuvette with dimensions 12.5 mm (L) × 12.5 mm (W) × 48 mm (H) with an optical path length of 10 mm. The recorded holograms were reconstructed with a step size of 20 µm between each other to cover a depth of 8 mm. One of the recorded holograms and a sample reconstruction are shown in Fig. 8(a) and (b), respectively. Using the procedure described in Section 3, 13 holograms were analyzed to identify 283 fibers. The resulting major and minor axes length distributions are shown in Fig. 8(c) and (d), respectively. The obtained mean major and minor axes length of these fibers were 138.74 and 13.34 µm, respectively.

The axis length distribution shown in Fig. 8(d) is indicative of the shape of the particles and can be used to classify particle shape. While spherical particles tend to lie close to the diagonal, needle shaped particles with a very high major to minor axis ratios tend to lie near the ordinate axis. This information is of importance for researchers interested in particle characterization and is typically not obtained in conventional particle analysis systems. From Fig. 8(d), the ALD clearly shows that the population contains needle shaped particles with similar widths but varying lengths.

5. Conclusions

In this paper, a particle size measurement methodology based on digital holographic microscopy was presented. The algorithm proposed for hologram processing is largely automated, but requires the selection of a few tuning parameters for particle segmentation. The effectiveness of the algorithm, however, is not very sensitive to these parameters, as shown through a series of experiments conducted for particles with different shapes, size ranges, and conditions. Even for the special case of randomly oriented fiber, the algorithm successfully measured the projected lengths with good accuracy, unless the fiber is long enough.

Hence, the size and shape measurements obtained using digital holography microscopy show good agreement with the given sizes and shapes measured using independent techniques. The results obtained in this study extend the potential of digital holography for applications in particle characterization and online monitoring of particulate processes.

Digital holography microscopy opens up promising possibilities in particle characterization including 3D measurements. Our future work will be directed at demonstrating the 3D measurements for non-symmetric particle population such as fibers and validation for false positives/negatives, etc. Besides these, digital holographic based technique deserves special attention in dealing with high suspension density, transparent and semi-transparent particles, which will also investigated in future.

References

Abbas, A., Nobbs, D., Romagnoli, J.A., 2002. Investigation of on-line optical particle characterization in reaction and cooling crystallization systems: current state of the art. Meas. Sci. Technol. 13 (3), 349–356.

Asundi, A., Singh, V.R., 2006. Circle of holography-digital in-line holography for imaging, microscopy and measurement. J. Holography Speckle 3 (2), 106–111.

Buraga-Lefebvre, C., Coetmellec, S., Lebrun, D., Ozkul, C., 2000. Application of wavelet transform to hologram analysis: three-dimensional location of particles. Opt. Laser Eng. 33 (6), 409–421.

Calderon De Anda, J., Wang, X.Z., Roberts, K.J., 2005. Multi-scale segmentation image analysis for the in-process monitoring of particle shape with batch crystallisers. Chem. Eng. Sci. 60 (4), 1053–1065.

Canny, J., 1986. A computational approach to edge detection. IEEE Trans. Pattern Anal. 8 (6), 679–698.

Darakis, E., Khanam, T., Rajendran, A., Kariwala, V., Asundi, A.K., Naughton, T., 2008. Processing of digital holograms for size measurements of microparticles. In: Asundi, A.K. (Ed.), Proceedings of the 9th International Symposium on Laser Metrology, vol. 715524. SPIE.

Denis, L., Fournier, C., Fournel, T., Ducottet, C., Jeulin, D., 2006. Direct extraction of the mean particle size from a digital hologram. Appl. Opt. 45 (5), 944–952.

Eggers, J., Kempkes, M., Mazzotti, M., 2008. Measurement of size and shape distributions of particles through image analysis. Chem. Eng. Sci. 63 (22), 5513–5521.

Frauel, Y., Naughton, T.J., Matoba, O., Tajahuerce, E., Javidi, B., 2006. Three-dimensional imaging and processing using computational holographic imaging. Proc. IEEE 94 (3), 636–653.

Hinsch, K.D., 2002. Holographic particle image velocimetry. Meas. Sci. Technol. 13 (7), R61.

Kempkes, M., Darakis, E., Khanam, T., Rajendran, A., Kariwala, V., Mazzotti, M., Naughton, T., Asundi, A.K., 2009. Three dimensional digital holographic profiling of micro-fibers. Opt. Exp. 17 (4), 2938–2943.

Kempkes, M., Eggers, J., Mazzotti, M., 2008. Measurement of particle size and shape by FBRM and in situ microscopy. Chem. Eng. Sci. 63 (19), 4656–4675.

Khanam, T., Darakis, E., Rajendran, A., Kariwala, V., Naughton, T., Asundi, A.K., 2008. On-line digital holographic measurement of size and shape of microparticles for crystallization processes. In: Asundi, A.K. (Ed.), Proceedings of the 9th International Symposium on Laser Metrology, vol. 71551k. SPIE.

Larsen, P.A., Rawlings, J.B., Ferrier, N.J., 2007. Model-based object recognition to measure crystal size and shape distributions from in situ video images. Chem. Eng. Sci. 62, 1430–1441.

Malkiel, E., Abras, J.N., Katz, J., 2004. Automated scanning and measurements of particle distributions within a holographic reconstructed volume. Meas. Sci. Technol. 15 (4), 601.

Onural, L., Ozgen, M.T., 1992. Extraction of three-dimensional object-location information directly from in-line holograms using Wigner analysis. J. Opt. Soc. Am. A 9 (2).

Patience, D.B., Rawlings, J.B., 2001. Particle-shape monitoring and control in crystallization processes. A.I.Ch.E. J. 47, 2125–2130.

Ruf, A., Worlitschek, J., Mazzotti, M., 2000. Modeling and experimental analysis of PSD measurements through FBRM. Part. Part. Syst. Char. 17 (4), 167–179.

Sarkar, D., Doan, X.-T., Ying, Z., Srinivasan, R., 2009. In situ particle size estimation for crystallization processes by multivariate image analysis. Chem. Eng. Sci. 64 (1), 9–19.

Schnars, U., Juptner, W., 2005. Digital Holography: Digital Hologram Recording, Numerical Reconstruction, and Related Techniques. Springer, Berlin.

Soontaranon, S., Widjaja, J., Asakura, T., 2008. Extraction of object position from in-line holograms by using single wavelet coefficient. Opt. Commun. 281 (6), 1461–1467.

Sun, H., Hendry, D.C., Player, M.A., Watson, J., 2007. In situ underwater electronic holographic camera for studies of plankton. IEEE J. Oceanic Eng. 32 (2), 373–382.

Vikram, C.S., 1992. Particle Field Holography. Cambridge University Press, Cambridge, UK.

Wang, X.Z., Roberts, K.J., Ma, C., 2008. Crystal growth measurement using 2d and 3d imaging and the perspectives for shape control. Chem. Eng. Sci. 63 (5), 1173–1184.

Winn, D., Doherty, M.F., 2000. Modeling crystal shapes of organic materials grown from solution. A.I.Ch.E. J. 46 (7), 1348–1363.

Xu, W., Jericho, M.H., Meinertzhagen, I.A., Kreuzer, H.J., 2002. Digital in-line holography of microspheres. Appl. Opt. 41 (25), 5367–5375.